Mechanism of growth inhibition by free bile acids in lactobacilli and bifidobacteria

Peter Kurdi, Koji Kawanishi, Kanako Mizutani, and Atsushi Yokota*

Laboratory of Microbial Resources and Ecology, Division of Applied Bioscience, Graduate School of Agriculture, Hokkaido University, Kita 9 Nishi 9, Kita-ku, Sapporo 060-8589, Japan.

*Corresponding author. Mailing address: Laboratory of Microbial Resources and Ecology, Division of Applied Bioscience, Graduate School of Agriculture, Hokkaido University, Kita 9 Nishi 9, Kita-ku, Sapporo 060-8589, Japan. Phone: +81-11-706-2501. Fax: +81-11-706-4961.

E-mail: yokota@chem.agr.hokudai.ac.jp.

Running Title: Mechanism of growth inhibition by free bile acids

ABSTRACT

The effects of the free bile acids (FBAs) cholic acid (CA), deoxycholic acid (DCA), and chenodeoxycholic acid (CDCA) on the bioenergetics and growth of lactobacilli and bifidobacteria were investigated. It was found that these FBAs reduced the internal pH levels of these bacteria in a rapid and stepwise kinetics and, at certain concentrations, dissipated ΔpH. The bile acid concentrations that dissipated ΔpH corresponded with the minimum growth inhibitory concentrations (MIC) for the selected bacteria. Unlike acetate, propionate, and butyrate, FBAs dissipated the transmembrane electrical potential (ΔΨ). In *Bifidobacterium breve* JCM 1192, the synthetic proton conductor pentachlorophenol (PCP), dissipated ΔpH in a slow and continuous kinetics at much lower concentration than FBAs, suggesting the different mode of action of FBAs from true proton conductors. Membrane damage assessed by fluorescent method and viability decrease were also observed upon exposure to CA or DCA at MIC, but not to PCP or short chain fatty acids mixture. Loss of potassium ion was observed at CA concentrations more than 2mM (0.4xMIC), while leakage of other cellular components increased at CA concentrations more than 4mM (0.8xMIC). Additionally, in experiments with extracted membrane phospholipid vesicles from *Lactobacillus salivarius* subsp, *salicinius* JCM 1044, CA and DCA at MIC collapsed the ΔpH with concomitant leakage of intra-vesicular fluorescent pH probe, while they did not show proton conductance at lower concentration range (e.g., 0.2xMIC). Taken together these observations, we conclude that FBAs at MIC disturb membrane integrity and this effect can lead to leakage of proton (membrane ΔpH and ΔΨ dissipation), potassium ion and other cellular components, and eventually cell

death.

INTRODUCTION

Bile, which is one of the most important host-derived factors to affect the indigenous intestinal microbiota, contains conjugated bile acids, i.e., free bile acids (FBAs) that are esterified by taurine or glycine. In the intestine, conjugated bile acids facilitate lipid digestion and absorption by emulsifying lipids. However, several indigenous intestinal microorganisms can enzymatically liberate the FBAs from conjugated bile acids (2). These FBAs are known to inhibit the growth of various intestinal microbes (3). Although this phenomenon was reported quite a long time ago, the mechanism of growth inhibition by FBAs and the details of the effects of these compounds on bacterial physiology have not been clarified. Moreover, knowledge of the mechanism underlying growth inhibition by FBAs is crucial in light of the development of probiotics that are capable of growing in the intestinal tract, in which FBAs are present at high concentrations.

Recently, we carried out transport experiments to show that cholic acid (CA), which is one of the FBAs, is accumulated in energized *Lactobacillus* and *Bifidobacterium* strains, where the transmembrane proton gradient (ΔpH, alkaline interior) is the driving force (11, 12). Since this accumulation must occur during bacterial growth in the intestine, growth inhibition may be associated with FBA accumulation. It has been proposed that the accumulation of CA, which is a hydrophobic weak acid with a pKa value of 6.4, is based on the diffusion of the protonated (neutral) CA molecules across the cell membrane, followed by their dissociation according to the ΔpH of the energized cells (11, 12). Since this process consumes ΔpH, the internal pH must be reduced. However, acidification of the internal pH by exogenously added FBAs has not been measured previously. Based on previous findings, growth inhibition by FBAs has been attributed to either acidification itself and/or ΔpH dissipation, which would lead to a deficiency in biological energy (proton motive force). Another possibility as a mechanism behind growth inhibition by FBAs is their potential membrane damaging effect. Therefore, in this study, we examined the bioenergetic consequences and the effect on membrane integrity upon the exposure of bacterial cells to FBAs, to elucidate the mechanism of growth inhibition by FBAs.

MATERIALS AND METHODS

Bacterial strains and chemicals. The microorganisms used in this study were obtained from the Japan Collection of Microorganisms (JCM, Wako, Japan). The strains were grown in half-strength (1/2) MRS medium (Becton Dickinson, Sparks, MD) at 37°C (except for *Lb. sakei* JCM 1157^T, which was cultured at 30^{o}C) under anaerobic conditions (mixed gas, N_2:CO_2:H_2; 8:1:1). In the case of the bifidobacteria, the medium was supplemented with 0.025% L-cysteine hydrochloride. The sodium salts of the FBAs were purchased from Sigma Chemical Co. (St. Louis, MO). Pentachlorophenol (PCP) was purchased from Aldrich Chemical Co. (Milwaukee, WI). Fluorescent dyes 5 (and 6-)-carboxyfluorescein diacetate succinimidyl ester (cFDASE) and 3,3'-dipropylthiadicarbocyanine iodide [$DiSC_3(5)$] were obtained from Molecular Probes, Inc. (Eugene, OR). Pyranin was the product of Acros Organics (Geel, Belgium). Other chemicals were of the highest quality commercially available.

Growth experiments. Bacteria were cultured in 1/2 MRS broth that contained various concentrations of FBAs, or other chemicals, under the conditions described above.

Bacterial growth was monitored periodically by measuring the absorbance of the culture broth at 660 nm. The minimum inhibitory concentration (MIC) for growth of each compound was determined as the lowest concentration that inhibited by 100% the growth of the test microorganism.

Intracellular pH measurement. The internal pH values of the lactobacilli and bifidobacteria were measured according to the method described previously (11), except that the experiments were performed with an external pH of 6.5, which is the pH of the 1/2 MRS broth. This method uses the internally conjugated fluorescent pH probe 5 (and-6-)-carboxyfluorescein, succinimidyl ester (cFSE). The exponential-phase cells cultured by the method described in "Bacterial strains and chemicals" were washed twice with 50mM potassium phosphate buffer (pH 6.5) containing 1mM $MgSO_4$ and 0.1 U/ml horseradish peroxidase (Buffer A). The cells were resuspended in 150mM potassium phosphate buffer (pH 6.5) containing 1mM $MgSO_4$ and 1.0 U/ml horseradish peroxidase (Buffer B) at an A_{660} of 0.5. The bacterial cells were preloaded with 4 μM of membrane-permeable precursor probe cFDASE, and incubated at appropriate temperatures (the same as the culture temperatures) for 30 min. During the incubation the precursor probe was cleaved by intracellular esterases, and the resulting cFSE molecules were conjugated to bacterial proteins. After centrifugation, cells were resuspended in the same volume of Buffer B, and the elimination of the unbound cFSE probe was conducted by the addition of glucose at a final concentration of 10 mM for 1 h at appropriate temperatures. The mixtures were centrifuged again and resuspended in Buffer B at an A_{660} of 0.5, and dispensed into a stirred and heated (at appropriate temperatures) cuvette holder of LS50B fluorimeter (PerkinElmer Life and Analytical Sciences Inc., Boston, MA). The internal pH of the bacteria was determined by measuring fluorescence intensities of the cell suspension with excitation and emission wavelengths of 490 and 520 nm, respectively (slit widths of 2.5 nm). During the measurement, energization with glucose and additions of various kinds of chemicals were conducted as described in the corresponding Figures and their legends. During pre-measurement preparations (e. g. probe loading, elimination of the unbound probe molecules) and in the cuvette throughout the internal pH measurements with the fluorimeter, an anaerobic atmosphere (mixed gas) was applied to prevent exposure of the cells to oxygen. Calibration of the fluorescent signal was carried out by measuring the fluorescence intensity of the de-energized cells at pH values between 4 and 10. The de-energization was conducted by the addition of 2 μM valinomycin plus 2 μM nigericin to the cell suspension.

Monitoring of the transmembrane electrical potential (ΔΨ). Changes in the membrane potentials of the lactobacilli and bifidobacteria upon energization and the addition of various chemical compounds were monitored using the cationic potential-sensitive fluorescent dye $DiSC_3(5)$, as reported previously (11), except that the experiments were carried out at external pH of 6.5. The cells cultured in the same manner as in the case of intracellular pH measurement were washed twice with 50mM potassium phosphate buffer (pH 6.5) containing 1mM $MgSO_4$ and 65 U/ml catalase (Buffer C), and resuspended in 150mM potassium phosphate buffer (pH 6.5) containing 1mM $MgSO_4$ and 65 U/ml catalase (Buffer D) at an A_{660} of 10. Then the cells were transferred to a stirred cuvette containing Buffer D and 0.5 μM $DiSC_3(5)$ at a final A_{660} of 0.05. The fluorescence intensity was monitored with LS50B fluorimeter (PerkinElmer) with excitation and emission wavelengths of 651 and 657 nm, respectively (slit widths of 4.0 nm). During measurements with the fluorimeter, mixed gas was introduced into the headspace of the cuvette, to ensure anaerobic conditions for the cells.

Membrane phospholipid extraction and membrane vesicle preparation. Cellular lipids were extracted by the modified Bligh & Dyer method (4). Approximately 4-5 g cell biomass (wet weight) was suspended in 5 ml deionized water and incubated with 20 mg/ml lysozyme at 37°C for about 6 h. The following steps were performed under N_2 to minimize oxidation. A methanol: chloroform (2:1, v/v) mixture (90 ml) was added to the cell suspension and stirred overnight at 4°C in the dark. The mixture was centrifuged (2000 × *g*, 5 min, 4°C), and the supernatant was collected, which was then stirred with 60 ml of a chloroform: water mixture (1:1) for 3 h. The mixture was allowed to stand until the phases separated. The chloroform phase was collected and centrifuged (2000 × *g*, 20 min, 4°C) to separate residual water. The chloroform-rich phase was collected again with a Pasteur pipette and the solvent was evaporated. The phospholipids from the total lipid extract were separated by a method that was based on the procedure described by Viitanen *et al.* (16). Dry lipids were dissolved in 1 ml chloroform; the mixture was dripped slowly into 80 ml ice-cold acetone, and stirred overnight in the dark. The mixture was centrifuged (2000 × *g*, 30 min, 4°C), the supernatant was removed, and the pellet was dried under an N_2 gas stream. The pellet was dissolved in 80 ml diethyl ether, and stirred for 1-2 h at room temperature. The mixture was centrifuged, and the supernatant was collected and evaporated. The extracted phospholipids were suspended in 1 ml of 50 mM (for experiments in Fig. 6) or 150 mM (for experiments in Fig. 5) potassium phosphate buffer (pH 6.5) that contained 1 mM pyranin. Small unilamellar vesicles were prepared by sonication for 30 min at 50 W. The vesicle suspension was centrifuged (20,000 × *g*, 10 min, 4°C) to remove metal particles. Untrapped pyranin was removed by gel filtration on a PD-10 column (Amersham Biosciences, Piscataway, NJ), and washed with 50 mM (for experiments in Fig. 6) or 150 mM (for experiments in Fig. 5) potassium phosphate buffer (pH 6.5). The internal pH changes of the pyranin-entrapped membrane vesicles were measured by pyranin fluorescence (excitation wavelength of 455 nm, emission wavelength of 509 nm with both excitation and emission slit widths of 15 nm) using LS50B fluorimeter (PerkinElmer). Calibration of the fluorescence signal was carried out as described previously (9).

Determination of the viability of *B. breve* JCM 1192 upon exposure to FBAs, PCP or short chain fatty acids mixture. Cells were cultured until mid-exponential phase in 1/2 MRS medium containing 0.025% L-cysteine hydrochloride at 37°C under anaerobic conditions. After harvesting, the cells were washed twice with sterile Buffer B and resuspended in the same buffer to an A_{660} of 0.5. Portions of this cell suspension were incubated with 10 mM glucose and each of the following chemicals: various concentrations of CA or DCA, 0.3 mM PCP or 117 mM short chain fatty acids (SCFAs, sodium acetate 66 mM, sodium propionate 26 mM, sodium butyrate 25 mM) mixture for 1 and 3 h. Cell suspension dilutions were made with sterile 0.85% NaCl solution and cells from appropriate dilutions were plated onto 1/2 MRS agar plates, which were incubated for 2 days in anaerobic jar at 37°C. Colonies were counted and the viabilities (%) were calculated based on the initial untreated cell suspension.

Determination of the membrane integrity of *B. breve* JCM 1192 upon exposure to FBAs, PCP or SCFAs mixture. We assessed membrane integrity changes of JCM 1192 in the presence of FBAs, PCP or SCFAs mixture by a fluorescent method based on membrane permeability of dead cells. This method can indicate the ratio of the cells with intact membranes in the population. Cell suspension (A_{660} of 0.3) was prepared and treated at the same conditions as in the plating method. After the treatment cells were subsequently incubated with a fluorescent dye mixture (Component A plus Component B) of LIVE/DEAD BacLight Bacterial Viability Kit (Molecular Probes) according to the manufacturer's recommendation for 15 min at 37°C. This kit contains the green fluorescent DNA dye SYTO 9 for all kinds of cells and the red fluorescent DNA dye Propidium Iodide for cells with compromised membrane. The cell suspensions were excited by 480 nm wavelength light and the emission spectrum between 490 and 700 nm were measured using LS50B fluorimeter (PerkinElmer) with both the excitation and emission slits set at 3.0 nm. Calibration used 100% live (no treatment) and 100% dead cells (treated with 100% isopropanol for 1 h). The ratio of the integrated intensity of the portion of each spectrum between 500-530 nm (green) to that between 620-650 nm (red) was calculated. To obtain a calibration curve the ratio of integrated green/red fluorescence was plotted versus the known percentage of live cells of the standard cell suspensions (10%, 50%, 90% live cell suspensions, prepared using 100% live and 100% dead cells).

Measurement of the leakage of cellular material from *B. breve* JCM 1192 upon exposure to FBAs. Cells were cultured until mid-exponential phase in 1/2 MRS medium containing 0.025% L-cysteine hydrochloride at 37°C under anaerobic conditions. After the harvest the cells were washed once with 50 mM sodium phosphate buffer (pH 6.5) containing 1 mM $MgSO_4$ and 1.0 U/ml horseradish peroxidase. Then the cells were resuspended in 150 mM sodium phosphate buffer (pH 6.5) containing 1 mM $MgSO_4$ and 1.0 U/ml horseradish peroxidase at an A_{660} of 0.5. The cell suspension was incubated at 37°C in the presence of 10 mM glucose and CA or DCA at the following concentrations (mM): CA at 0.1, 0.5, 1, 2, 4, 6, 8, 15, 20 or DCA at 0.01, 0.05, 0.1, 0.2, 0.4, 0.6, 0.8, 1, 2. Samples at various time intervals (up to 3 h) were taken from the reaction mixtures and centrifuged twice at 20,000 × *g* for 5 min. Then the supernatants were used for further studies. The absorbance of the supernatants at 260 and 280 nm of the CA treated samples were measured with a Beckman DU 640 Spectrophotometer (Beckman Coulter, Inc., Fullerton, CA). For the measurement of potassium leakage portions of the supernatants were treated with 1 N $HClO_4$ (1:1) for overnight at room temperature. Then the mixtures were diluted 2.5-fold with 0.36 N HCl and centrifuged at 1350 × *g* for 10 min. The potassium amounts in the supernatants were then measured by flame atomic absorption spectroscopy (Z-5310 Polarized Zeeman Atomic Absorption Spectrophotometer, Hitachi High-Technologies Corp. Japan).

RESULTS

The MIC values for FBAs correspond with their ΔpH-dissipating concentrations in many lactobacilli and bifidobacteria. The MIC values that were obtained for CA and DCA using selected lactobacilli and bifidobacteria are shown in Table 1. The MIC of CA ranged from 3.0 to 13.0 mM, which was about ten-times higher than the MIC of DCA (0.3-0.8 mM). In our previous report (11), we showed that an SCFAs mixture reduced the ΔpH of *B. breve* JCM 1192. Therefore, we expected that FBAs, such as CA and DCA, which are also weak acids, might have similar effects on the internal pH of this microorganism. The finding that CA is accumulated in energized lactobacilli and bifidobacteria by a ΔpH-driven diffusion mechanism (11, 12) led us to expect that the FBAs would acidify the cytoplasm of these bacteria. Indeed, we observed a decrease in ΔpH following the addition of FBAs in JCM 1192, as shown in Fig. 1ab. However, this reduction turned to total dissipation of ΔpH at certain bile acid concentrations, which was confirmed by the finding that the addition of nigericin (an ionophore known to dissipate ΔpH) had no further effect on the internal pH of JCM 1192. Surprisingly, the ΔpH-dissipating concentrations of CA and DCA closely paralleled the MIC values of these FBAs in many lactobacilli and bifidobacteria (Table 1). Moreover, we observed an approximately ten-fold difference between the ΔpH-dissipating concentrations of CA and DCA, with a similar difference being observed between their MIC values (Table 1). In addition, it was found that CDCA dissipated the ΔpH of JCM 1192 at a similar concentration to DCA (0.4 mM; Fig. 1c), which was also similar to the MIC value of CDCA (0.5 mM; data not shown in Table1). In contrast, the SCFAs mixture, which reduced the internal pH of JCM 1192 (11), had no growth inhibitory effect on this bacterium, even when individual SCFAs alone were applied up to 400 mM concentration (data not shown).

FBAs, but not SCFAs are able to dissipate ΔΨ. It has been reported that acetic acid is accumulated in *Streptococcus bovis* cells (15), which results in a reduction of the intracellular pH. In *Clostridium thermoaceticum*, acetate caused some decrease in ΔpH, but this decrease was partially compensated by an increase in ΔΨ (1). However, the effect of SCFAs on ΔΨ, especially in the enteric species of lactobacilli and bifidobacteria, has not been demonstrated previously. The cationic fluorescent probe $DiSC_3(5)$ was used to monitor ΔΨ, as indicated by the fluorescence quenching. The results show that the addition of any of three SCFAs (sodium acetate, sodium propionate, and sodium butyrate) to energized JCM 1192 cells decreased the fluorescent signal, which indicated an increase of ΔΨ (Fig. 2). The existence of ΔΨ after the addition of SCFAs was confirmed by the addition of valinomycin, which is an ionophore that dissipates ΔΨ, resulting in a sharp increase in probe fluorescence. All three FBAs had the opposite effect to that of the SCFAs, since they dissipated the ΔΨ of JCM 1192 at certain concentrations (Fig. 3). The dissipation of ΔΨ by bile acids was verified by the fact that subsequent addition of valinomycin did not cause any further increase in the fluorescence intensity. Similar to the ΔpH dissipation results, we observed that the concentration required to dissipate ΔΨ was approximately ten-fold lower for DCA and CDCA than for CA; this tendency also held true for other strains, at least in the case of DCA (Table 1). Although the

ΔpH-dissipating concentrations of the FBAs were found to be somewhat higher than the ΔΨ-dissipating concentrations (Table 1), this may be attributed to the fact that the cell densities were higher during the ΔpH measurements (A_{660}=0.5) than during the ΔΨ measurements (A_{660}=0.05).

The kinetics of ΔpH dissipation by a synthetic proton conductor, PCP appear to be different from that by FBAs in *Lb. salivarius* subsp. *salicinius* JCM 1044 and *B. breve* JCM 1192. Compounds that can simultaneously dissipate ΔpH and ΔΨ are called proton conductors. We compared the effects of FBAs and a known proton conductor PCP on the bioenergetics of *Lb. salivarius* subsp. *salicinius* JCM 1044. As expected, PCP dissipated the ΔΨ and ΔpH of JCM 1044 but at lower concentrations than FBAs (Fig. 4). However, the kinetics of ΔpH dissipation was not stepwise as in the case of FBAs (Fig. 1) but it rather followed a continuously decreasing curve (Fig. 4b). In addition, similar ΔΨ and ΔpH-dissipation kinetics was observed when PCP was added to energized JCM 1192 (data not shown). The observed relatively slower, but gradual ΔpH-dissipation kinetics is probably reflecting the PCP and PCP-anion's recycling transmembrane movement, which ultimately leads to the dissipation of the transmembrane proton concentration gradient. Therefore, these data indicate that the apparent proton conductive mode of action of FBAs is possibly different from true proton conductors.

Exposure to CA or DCA increases membrane damage and decrease viability in *B. breve* JCM 1192. We investigated the membrane integrity and viability of JCM 1192 upon exposure to FBAs by a fluorescent method and the conventional plate-out method, respectively, with PCP and SCFAs as references. As shown in Table 2, CA and DCA showed decreasing membrane integrity and decreasing viability with increasing concentrations of CA or DCA. In contrast the proton conductor PCP and SCFAs treatment caused no serious membrane damage and viability loss even over 3 h except that the viability dropped remarkably after 3 h in the case of PCP treatment (Table 2). This indicates the importance of proton motive force (cellular energy) on the viability of the bacterial cell. PCP, while possibly not affecting the membrane integrity, cause viability loss presumably by its proton conductance leading to serious cellular energy shortage (Fig. 4) after 3 h. It should be noted that in the case of CA and DCA at concentrations more than 4 mM and 0.4 mM, respectively, we detected much less viability by plate-out method than membrane integrity reduction detected by the fluorescent method (Table 2).

The different effects of PCP and FBAs in isolated membrane lipid vesicles indicate different mode of action. Proton conductors share the characteristic that they can cross membrane bilayers in both the protonated (neutral) and anionic forms. However, previous studies indicated that bile acid anions traverse phosphatidylcholine membranes very slowly (5). Therefore, we extracted the membrane phospholipids from JCM 1044, to test the proton conductive properties of FBAs on these membrane vesicles. In these experiments, we added KOH to the vesicle suspension, creating a ΔpH of approximately 0.3 pH unit across the vesicle membrane. The addition of KOH instantly increased the external pH of the vesicle suspension from about 6.5 to 6.8. The external addition of KOH resulted in a fast, sharp increase in intravesicular pH, followed by a slower pH increase, which indicated slow leakage of H^+/OH^- across the membrane bilayer (Fig. 5). When PCP was added after the KOH, it caused a small decease in intravesicular pH, followed by a decrease in the pre-existing ΔpH to near zero within a few minutes (Fig. 5a). The internal acidification immediately after the addition of PCP may be attributed to transbilayer movement of the neutral (protonated) form, followed by dissociation inside the vesicles, which results in an increase in the intravesicular proton concentration. Similar events were observed by adding CA at 3.5 mM (Fig. 5b) or DCA at 0.4 mM (Fig. 5c) to the vesicles, which also led to a substantial decrease of ΔpH (increasing internal pH). These results suggest that FBAs can increase the H^+/OH^- leakage across the membrane bilayer, although at a lower rate than PCP. However, when ΔpH dissipating concentrations (for JCM 1044) of CA (7 mM) or DCA (0.8 mM) were added (Fig. 5b, c), pre-existing ΔpH instantly disappeared similar to the effect of nigericin (Fig. 5a). This latter sudden dissipation of ΔpH was not observed in the case of PCP, suggesting a different action mechanism of CA and DCA from that of proton conductors. In contrast, when lower concentrations of CA (1 to 2 mM) or DCA (0.1 to 0.2 mM) were added to membrane vesicles the H^+/OH^- leakage did not visibly increase as shown in Fig. 6. Furthermore, our experiments with membrane vesicles from JCM 1192 produced similar results (data not shown). Additionally, when membrane vesicles of JCM 1192 were ultracentrifuged (135,000 x *g*, 30 min) after 6.0 mM CA or 0.8 mM DCA treatment, almost all of the total pyranin fluorescence was found in the supernatant, indicating severe membrane damage. While, about 50% of the total pyranin fluorescence was detected in the supernatant of untreated vesicles. These data imply that after the addition of 7.0 mM CA or 0.8 mM DCA parallel with H^+/OH^- leakage pyranin leakage was possibly also occurred (Fig. 5b, c). Therefore, our results suggest that FBAs at certain concentrations ([CA]>2 mM, [DCA]>0.2 mM) disturb membrane integrity in *Lactobacillus* and *Bifidobacterium* cells, which leads to the collapse of the transmembrane proton gradient.

Exposure to FBAs leads to leakage of cytoplasmic potassium in a concentration dependent manner and can result in leakage of cytoplasmic proteins when CA concentration increased further. To test the increase of the permeability of ions other than proton caused by membrane damage, we measured the amount of potassium released into $NaPO_4$ buffer upon CA exposure from JCM 1192. The results showed that 15 min (Fig 7a) exposure to 4-6 mM CA caused the leakage of almost all cytoplasmic potassium. Similar results were also obtained at 5 min and 3 h exposure (data not shown). Similar pattern of potassium leakage was obtained with DCA, where 0.4-0.6 mM DCA resulted in the maximum potassium permeability of the cell membrane (data not shown). These results imply that all ions are possibly instantly permeable to the membrane in the presence of 4-6 mM CA (or 0.4-0.6 mM DCA), and they are in good agreement with MIC and ΔpH dissipating concentrations of CA (or DCA) in JCM 1192. On the other hand, this CA concentration range did not lead to near maximum UV absorbance values (at 260 and 280 nm) by macromolecules, which were observed at exposures to 15-20 mM CA (Fig 7b). We measured near zero UV absorbance values up to 2 mM CA, and the absorbancies started to increase substantially at higher concentrations. In contrast to potassium ion leakage, UV absorbance values at every CA concentrations were increasing as the function of time (data not shown), resulting in the highest absorbance values at the longest tested exposure time 3 h. Additionally, we observed detectable protein bands on the SDS-PAGE of cell free supernatant at CA concentrations of 15 and 20 mM after 3 h exposure (data not shown).

DISCUSSION

In recent years, lactobacilli and bifidobacteria have been studied intensively and used frequently as probiotics. When used as probiotics and as members of the human indigenous intestinal microbiota, these lactic acid bacteria have to cope with the challenge of FBAs. In our previous reports, we noted that energized bifidobacteria accumulated CA, which is one of the most abundant FBAs in humans, when the extracellular concentration of CA was within the physiological range of up to 2 mM (11). The mechanism of accumulation of the weak acid CA was found to be similar to the accumulation of other weak acids, e.g., acetate, in some bacteria (15). The accumulation of weak acids in bacteria generally involves transbilayer diffusion of the neutral, protonated weak acid, followed by its intracellular dissociation, thereby lowering the internal pH. However, internal pH drop as a consequence of weak acid accumulation, as shown in previous studies (1, 6), has not been demonstrated previously with CA in lactobacilli or bifidobacteria. The results presented here (Fig. 1) demonstrate a decrease in the internal pH in response to the addition of FBAs; they also show total dissipation of the ΔpH. Moreover, the concentrations of FBAs required for ΔpH dissipation corresponds with the minimum concentrations of FBAs that abrogate the growth *in vitro* of lactobacilli and bifidobacteria (MIC, Table 1). In addition, MIC and ΔpH dissipating concentrations determined in this study are (with one exception) lower than the critical micellar concentrations of either CA (11 mM), DCA (3 mM) or CDCA (4 mM) (14). Our results also showed that unlike acetate, propionate, and butyrate (Fig. 2), FBAs can also dissipate ΔΨ (Fig. 3) of intact cells. To our knowledge, this is the first time that growth inhibition by FBAs has been linked to a bioenergetic factor, suggesting that dissipation of proton motive force is involved in this mechanism.

Our data also showed a significant (about ten-fold) difference between the MIC values and ΔpH-dissipating concentrations of CA and DCA, which cannot be attributed simply to the subtle difference in their pK_a values (6.4 and 6.58 for CA and DCA, respectively). It has been reported that transbilayer movement (flip-flop) in small unilamellar vesicles is at least ten-times faster for the more hydrophobic (8) DCA and CDCA compounds (both have two OH functional groups) than for CA (three OH groups) (10). This implies that ten-times more DCA and CDCA molecules can cross the membrane, in a certain time, than can CA molecules. Thus, if CA is present at a concentration that is ten-times higher than that of DCA or CDCA, the same number of molecules of all three species will permeate the membrane within the same time period. This may explain the almost ten-fold differences between CA and DCA in terms of MIC and ΔpH-dissipating concentrations.

The mechanism of the proton conductance of FBAs (Figs. 1 and 3, Table 1) was suggested to be different from that of PCP, a synthetic proton conductor, by the observed different kinetics of ΔpH dissipation. The kinetics of ΔpH dissipation in energized cells of *B. breve* JCM 1192 by FBAs was stepwise (Fig. 1), which is in contrast to PCP with kinetics of continuous, steady decrease (Fig. 4) probably resulting from its recycling mode of action. In experiments using extracted membrane phospholipid vesicles (Fig. 5), we found that at certain concentrations (3.5 mM CA or 0.4 mM DCA) FBAs behave similarly to the PCP, but at higher concentrations (7.0 mM CA or 0.8 mM DCA) FBAs instantly dissipated ΔpH (Fig. 5b, c), while ΔpH dissipation by PCP was continuous and not immediate (Fig. 5a). These observations did not contradict the experiments using small unilamellar phosphatidylcholine vesicles, in which FBAs did not show proton conductor-like behaviors (10). In those experiments, where eukaryotic membrane constituent phosphatidylcholine was used, bile acids were applied only up to concentrations of 0.2 mM at which we observed no proton conductor-like behavior by CA or DCA (Fig. 6). NMR data have also indicated that the transmembrane movement of bile acid anions is very slow in unilamellar vesicles (5).

The gradual decrease of membrane integrity as demonstrated by fluorescent dye staining with increasing concentrations of FBAs but not with PCP or SCFAs mixture (Table 2) may suggest that the proton conductor like action of FBAs is associated with membrane damage.

This notion was strengthened by the results of vesicle experiments in which instant dissipation of ΔpH was observed by the challenge of 7.0 mM CA or 0.8 mM DCA (Fig. 5b, c). Under these conditions FBAs damage the membrane to the extent that it becomes freely permeable to H^+/OH^- and possibly even to pyranin. Detection of nearly maximum leakage of potassium ion from intact cells of JCM 1192 upon exposure to 4 to 6 mM CA (Fig. 7a) or 0.4 to 0.6 mM DCA also indicated that the increased ion peameability is not specific to proton but ions in general. A recent finding that CA at a concentration near to our MIC values increased the uptake of the aminoglycoside gentamicin by 18-fold in *Lb. plantarum* WCFS-1 (7) supports the notion that, beside ions, at least small molecular weight metabolites (those having molecular weights similar to gentamicin and pyranin, ca. 400-500) might also cross the membrane when CA is present in MIC range. The increase of UV absorbance (Fig. 7b) was more pronounced at CA concentrations of 15 to 20 mM, where membrane damage seems severe enough to let the cell proteins to leak out. Although the precise mechanism that results in membrane permeability is not clear, we can assume that free bile acids integrate into the phospholipid bilayer to disorder membrane functions leading to the permeability increase. In the equilibration, DCA can be integrated into the membrane much more effectively than CA since its partition coefficient (wt % of DCA bound to phosphatidylcholine vesicles/ wt % of DCA in water) was found 3.5 times higher than that of CA (10).

An important finding with the membrane integrity and viability check was that viabilities obtained with plate-out method gave much lower values than membrane damage assessed by fluorescent method at CA and DCA concentrations more than 4 mM and 0.4 mM, respectively (Table 2). This discrepancy may suggest that increased ion permeability due to the decreased membrane integrity below threshold value may determine the viability of the cell.

Under such conditions (Table 2, CA at 4 mM), while membrane integrity is not very low (47-62%) but the viability is lost dramatically (0.14-0.86%) due to the dissipation of proton motive force (Fig. 1a, Fig. 3a) and loss of homeostasis of potassium ion distribution across the cell membrane (Fig. 7a). Taken together these observations, the mechanism of FBAs to inhibit bacterial growth is concluded to be their membrane damaging effect leading to the dissipation of concentration gradient of proton, potassium and probably other ions across the membrane and also the leakage of small molecular weight metabolites from the cell. As the consequence, the bacterial cell may lose not only proton motive force (energy), but also important ions and solutes from the cytosol, thereby leading to the growth inhibition and viability loss as the incubation time increases. Based on this hypothesis, the observed increase of UV absorbance (Fig 7b) probably due to the leakage of cellular proteins is not directly involved in the mechanism of growth inhibition. In sharp contrast, our data clearly demonstrated that PCP and SCFAs do not affect membrane integrity (Fig. 2, Table 2) and hence viabilities. This would also explain the result of no growth inhibition by SCFAs.

Our previous findings (11,12) that energized *Lactobacillus* and *Bifidobacterium* strains accumulate CA intracellularly are not in conflict with the membrane integrity disturbance mechanism outlined above. The extracellular concentration of CA in our earlier transport experiments was 0.1 mM (up to 2 mM), which is substantially lower than that for complete dissipation of ΔpH (Fig. 1a) with high membrane integrity (Table 2). Under these concentrations, CA molecule generally behaves as a weak acid, distributing across the membrane according to the membrane ΔpH. Based on the above shown evidences, we can propose a concentration dependent mode of action of CA to cells of lactobacilli and bifidobacteria: CA is accumulated into the energized cells at external concentrations at around 0.1 mM (up to 2 mM).

CA provokes membrane damage at 2 to 4 mM range leading to increased peameability of ions and metabolites. Complete dissipation of proton motive force and the collapse of other ion concentration gradient(s) as well as probably the leakage of cellular metabolites take place at concentrations around MIC, where viability of the cell is dramatically decreased. When much higher concentration of CA is applied (up to 20 mM), UV-absorbing cellular materials as represented by proteins are leaking out.

The results presented in this study strongly suggest that in the human intestine the populations of lactobacilli and bifidobacteria are controlled in part by the concentrations of FBAs. Probiotic lactic acid bacteria accumulate CA (or probably DCA as well) when its concentration is not so high with mild viability decrease. On the other hand, apparent proton conductance and severe membrane permeability disturbance can occur when CA or DCA concentrations in the human gut become higher than threshold values. For example, concentrations of up to 0.3 mM DCA have been detected in the fecal water of healthy subjects (13) and estimation from viability and membrane damage data in Table 2 suggests a possibility that this compound exerts considerable inhibition of bacterial growth in the human intestine.

ACKNOWLEDGEMENTS

Peter Kurdi and this project were supported in part by a Postdoctoral Fellowship (P04199) from the Japan Society for Promotion of Science. The authors thank Mr. Hiroki Matsubara for his assistance in the experiments.

REFERENCES

1. **Baronofsky, J. J., W. J. A. Schreurs, and E. R. Kashket.** 1984. Uncoupling by acetic acid limits growth of and acetogenesis by *Clostridium thermoaceticum*. Appl. Environ. Microbiol. **48:**1134-1139.
2. **Baron, S. F., and P. B. Hylemon.** 1997. Biotransformation of bile acids, cholesterol, and steroid hormones, p. 470-510. *In* R. I. Mackie, and B. A. White (ed.), Gastrointestinal microbiology vol. I. Gastrointestinal ecosystems and fermentations. International Thomson Publishing, New York, N. Y.
3. **Binder, H. J., B. Filburn, and M. Floch.** 1975. Bile acid inhibition of intestinal anaerobic organisms. Am. J. Clin. Nutr. **28**:119-125.
4. **Bligh, E. G, and W. J. Dyer.** 1959. A rapid method of total lipid extraction and purification. Can. J. Biochem. Physiol. **37:**911-917.
5. **Cabral, D. J., D. M. Small, H. S. Lilly, and J. A. Hamilton.** 1987. Transbilayer movement of bile acids in model membranes. Biochemistry **26:**1801-1804.
6. **Diez-Gonzalez, F., and J. B. Russell.** 1997. Effects of carbonylcyanide-*m*-chlorophenylhydrazone (CCCP) and acetate on *Escherichia coli* O157:H7 and K-12: uncoupling versus anion accumulation. FEMS Microbiol. Lett. **151:**71-76.
7. **Elkins, C. A., and L. B. Mullis.** 2004. Bile-mediated aminoglycoside sensitivity in *Lactobacillus* species likely results from increased membrane permeability attributable to cholic acid. Appl. Environ. Microbiol. **70:**7200-7209.
8. **Heuman, D. M.** 1989. Quantitative estimation of the hydrophilic-hydrophobic balance

of mixed bile salt solutions. J. Lipid Res. **30:**719-730.

9. **Kamp, F., and J. A. Hamilton.** 1992. pH gradients across phospholipid membranes caused by fast flip-flop of un-ionized fatty acids. Proc. Natl. Acad. Sci. USA **89:**11367-11370.

10. **Kamp, F., and J. A. Hamilton.** 1993. Movement of fatty acids, fatty acid analogues, and bile acids across phospholipid bilayers. Biochemistry **32:**11074-11086.

11. **Kurdi, P., H. Tanaka, H. W. van Veen, K. Asano, F. Tomita, and A. Yokota.** 2003. Cholic acid accumulation and its diminution by short-chain fatty acids in bifidobacteria. Microbiology **149:**2031-2037.

12. **Kurdi, P., H. W. van Veen, H. Tanaka, I. Mierau, W. N. Konings, G. W. Tannock, F. Tomita, and A. Yokota.** 2000. Cholic acid is accumulated spontaneously, driven by membrane ΔpH, in many lactobacilli. J. Bacteriol. **182:**6525-6528.

13. **Rafter, J. J., and C. Branting.** 1991. Bile acids — interaction with the intestinal mucosa. Eur. J. Cancer Prev. **1 (Suppl. 2):**49-54.

14. **Roda, A., A. F. Hofmann, and K. J. Mysels.** 1983. The influence of bile salt structure on self-association in aqueous solutions. J. Biol. Chem. **258:**6362-6370.

15. **Russell, J. B.** 1991. Resistance of *Streptococcus bovis* to acetic acid at low pH: relationship between intracellular pH and anion accumulation. Appl. Environ. Microbiol. **57:**255-259.

16. **Viitanen, P., M. J. Newman, D. L. Foster, T. H. Wilson, and H. R. Kaback.** 1986. Purification, reconstitution, and characterization of the *lac* permease of *Escherichia coli*. Methods Enzymol. **125:**429-452.

FIGURE LEGENDS

Fig. 1. Effects of CA (a), DCA (b) and CDCA (c) on the internal pH of *B. breve* JCM 1192. Cells (A_{660}~0.5) were preloaded with cFSE and energized with 10 mM glucose in Buffer B. The respective FBAs were then added to the indicated final concentrations. Nigericin (200 nM) was added to check the dissipation of the ΔpH. The data shown in this and the following figures are representative of at least three experiments that gave similar results.

Fig. 2. Effects of sodium acetate (a), sodium propionate (b), and sodium butyrate (c) on the membrane potential of *B. breve* JCM 1192. Washed cells (A_{660}~0.05) were added to the cuvette, which contained the $DiSC_3(5)$ probe (0.5 μM) in Buffer D. The cells were energized with glucose (10 mM), followed by the addition of the respective SCFAs at the indicated final concentrations. Valinomycin (5 nM) was added to check the dissipation of the ΔΨ. The fluorescence intensity is expressed in arbitrary units (a.u.).

Fig. 3. Effects of CA (a), DCA (b), and CDCA (c) on the membrane potential of *B. breve* JCM 1192. The experimental procedures were the same as those described in the legend to Fig. 2, except that respective FBAs were added instead of SCFAs, at the indicated final concentrations.

Fig. 4. Effects of PCP on the membrane potential (a) and internal pH (b) of *Lb. salivarius* subsp. *salicinius* JCM 1044. (a) The experimental procedures were the same as those described in the legend to Fig. 2, except that PCP was added instead of SCFAs at the indicated final concentrations. (b) The experimental procedures were the same as those described in the

legend to Fig. 1, except that PCP was added instead of FBAs at the indicated final concentrations.

Fig. 5. Effects of PCP (a), CA (b), and DCA (c) on the internal pH of membrane vesicles of *Lb. salivarius* subsp. *salicinius* JCM 1044. An artificial ΔpH was established by the addition of 28 μl of 2N KOH to the membrane vesicle suspension in 2 ml of 150 mM potassium phosphate buffer, which altered the external pH from 6.5 to about 6.8. The chemical compounds were added at the indicated final concentrations. Nigericin (100 nM) was added to dissipate the pre-existing ΔpH.

Fig. 6. Effects of lower concentrations of CA (a), and DCA (b) on the internal pH of membrane vesicles of *Lb. salivarius* subsp. *salicinius* JCM 1044. Artificial ΔpH was established by the addition of 10 μl 2N KOH to the membrane vesicle suspension in 2 ml 50 mM potassium phosphate buffer, which altered the external pH from 6.5 to about 6.8. The other experimental conditions were the same as those described in legend to Fig. 5.

Fig. 7. Measurement of the leakage of K^+ (a) and other cellular materials (b) from *B. breve* JCM 1192 upon exposure to CA for 15 min (a) and 3 h (b). Cells (A_{660}~0.6) were incubated with various concentrations of CA in 150 mM sodium phosphate buffer (pH 6.5) containing 1 mM $MgSO_4$, 1.0 U/ml horseradish peroxidase and 10 mM glucose. The K^+ concentration (a) and the UV absorbance (b) at 260 nm (●) and 280 nm (○) of the cell free supernatant were determined spectroscopically.

Table 1. CA and DCA concentrations that totally inhibit growth and dissipate the ΔpH and ΔΨ in lactobacilli and bifidobacteria

Strain	Origin	CA (mM)			DCA (mM)		
		MIC	ΔpH diss.	ΔΨ diss.	MIC	ΔpH diss.	ΔΨ diss.
Lactobacillus acidophilus JCM 1034	Human intestine	8.5	5.5	ND	ND	ND	ND
Lb. salivarius subsp. *salicinius* JCM 1040	Human intestine	6.0	5.0	ND	0.6	0.8	ND
Lb. salivarius subsp. *salicinius* JCM 1044	Human intestine	6.0	7.0	3.0	0.7	0.8	0.3
Lb. salivarius subsp. *salicinius* JCM 1047	Swine intestine	4.5	8.0	ND	0.55	0.9	ND
Lb. gasseri JCM 1131^T	Human intestine	7.0	6.5	3.5	ND	1.0	0.7
Lb. reuteri JCM 1112^T	Intestine of adult	13.0	10.0	4.0	ND	0.7	0.4
Lb. salivarius subsp. *salivarius* JCM 1231^T	Human saliva	5.5	6.5	ND	ND	ND	ND
Lb. buchneri JCM 1115^T	Tomato pulp	6.5	6.0	ND	0.8	0.8	ND
Lb. sakei JCM 1157^T	Starter of sake	4.0	9.0	3.0	0.7	0.9	0.2
Bifidobacterium breve JCM 1192^T	Intestine of infant	5.0	6.0	2.0	0.5	0.6	0.3
B. breve JCM 7017	Human feces	3.0	6.0	ND	0.55	0.6	ND
B. psudocatenulatum JCM 1200^T	Feces of infant	3.0	6.0	3.0	0.45	0.6	0.3
B. gallicum JCM 8224^T	Human feces	7.0	8.0	ND	0.45	0.8	ND
B. longum JCM 1217^T	Intestine of adult	9.0	8.0	3.0	0.55	0.6	0.2
B. bifidum JCM 1255^T	Feces of infant	5.0	4.0	ND	0.3	0.4	ND
B. adolescentis JCM 1275^T	Intestine of adult	5.0	8.0	ND	0.4	0.6	ND

All of the data are the means of two separate experiments. ND, Not determined.

Table 2. Monitoring of membrane integrity and viability of *B. breve* JCM 1192 upon exposure to bile acids, PCP and SCFA mixture

Treatment		Membrane integrity by fluorescent method (%)		Viability by plate-out method (%)	
		1 h	3 h	1 h	3 h
CA	0.1 mM	87.9±5.29	93.12±13.51	112.5±12.02	106.4±16.33
	1 mM	92.68±5.73	90.71±1.22	49.85±8.84	14.5±1.41
	2 mM	88.53±12.41	89.04±1.36	14.67±2.83	3.96±2.06
	4 mM	47.56±6.07	62.00±13.66	0.86±0.06	0.14±0.04
	6 mM	14.19±3.54	18.73±0.19	0.16±0.11	0.03±0.01
	8 mM	13.63±0.52	18.31±3.42	0.03±0.02	0.006±0.003
DCA	0.01 mM	75.10±5.87	68.51±3.80	111.0±17.0	101.61±5.23
	0.1 mM	67.15±18.35	58.97±2.30	82.39±14.83	67.65±3.61
	0.2 mM	67.60±18.34	60.24±8.89	42.42±4.41	27.46±14.35
	0.4 mM	27.08±4.06	32.09±5.52	4.06±2.50	0.19±0.09
	0.6 mM	6.11±2.67	6.44±1.81	0.10±0.04	0.05±0.02
	0.8 mM	4.47±0.19	7.77±0.17	0.007±0.003	0.002±0.001
PCP	0.3 mM	72.10±17.35	92.20±2.19	88.86±27.29	0.83±0.75
SCFA	117 mM	91.73±2.34	84.17±3.50	33.18±16.33	39.39±3.89

Results are shown as means±SD where n≥2.

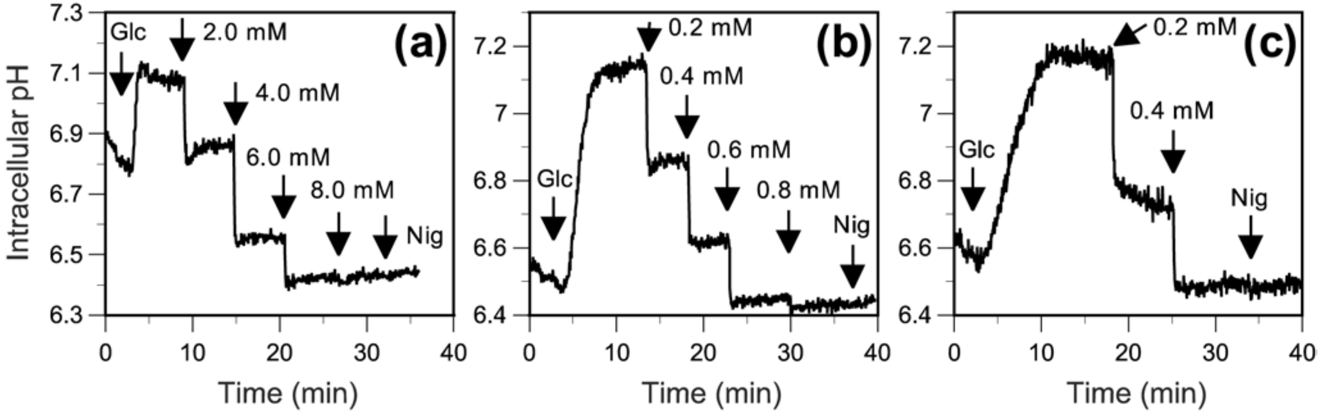

(a)
(b)
(c)
Intracellular pH
Time (min)
Glc
2.0 mM
4.0 mM
6.0 mM
8.0 mM
Nig
0.2 mM
0.4 mM
0.6 mM
0.8 mM

Fig. 1.

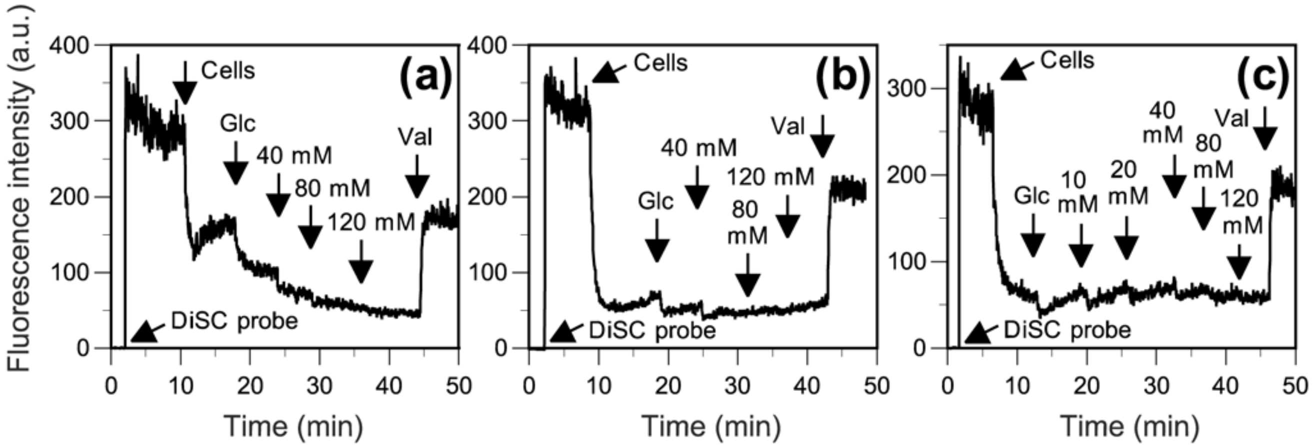

Fluorescence intensity (a.u.)
Time (min)
(a)
Cells
Glc
40 mM
80 mM
120 mM
Val
DiSC probe
(b)
Cells
40 mM
Val
Glc
120 mM
80 mM
DiSC probe
(c)
Cells
40 mM
Val
80 mM
Glc
10 mM
20 mM
120 mM
DiSC probe

Fig. 2.

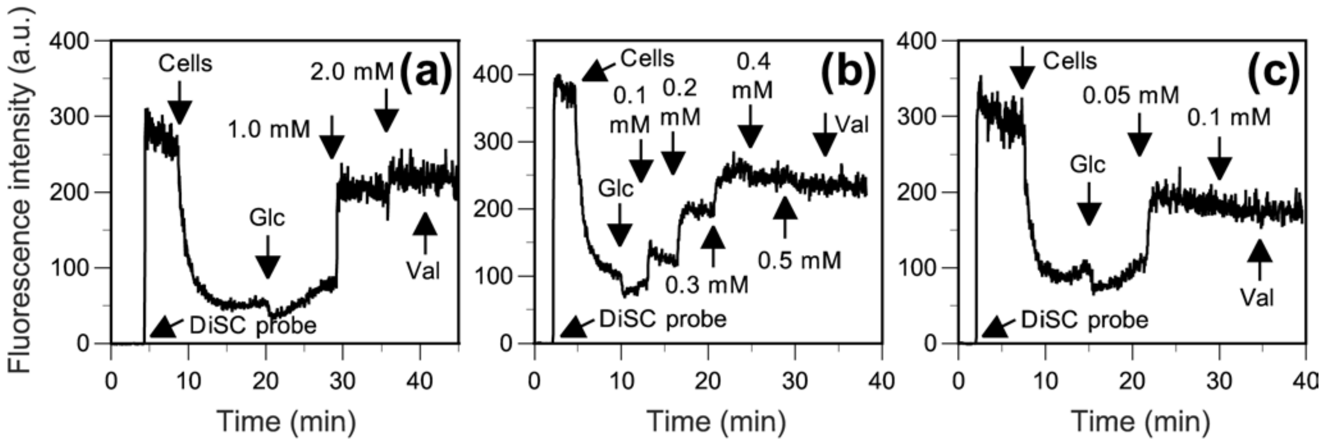

Fluorescence intensity (a.u.)
Cells
2.0 mM
(a)
1.0 mM
Glc
Val
DiSC probe
Time (min)
(b)
0.1 mM
0.2 mM
0.4 mM
Val
Glc
0.3 mM
0.5 mM
(c)
0.05 mM
0.1 mM

Fig. 3.

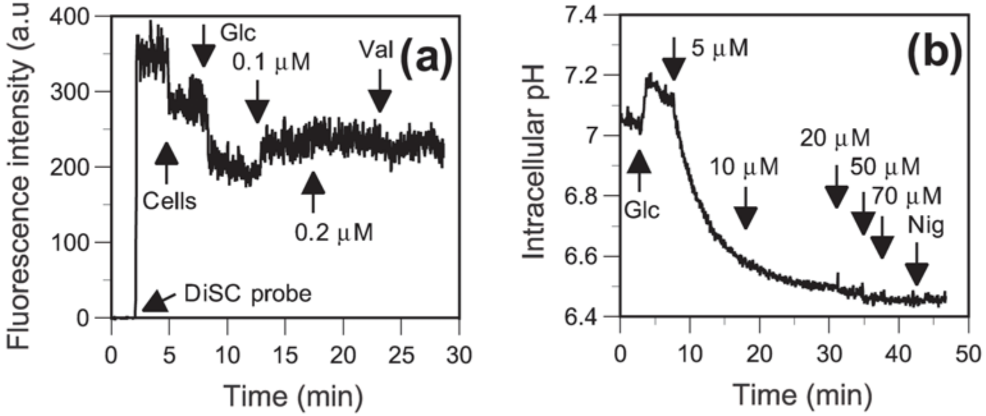

(a)
Fluorescence intensity (a.u.)
Glc
0.1 μM
Val
Cells
0.2 μM
DiSC probe
Time (min)
(b)
Intracellular pH
5 μM
Glc
10 μM
20 μM
50 μM
70 μM
Nig
Time (min)

Fig. 4.

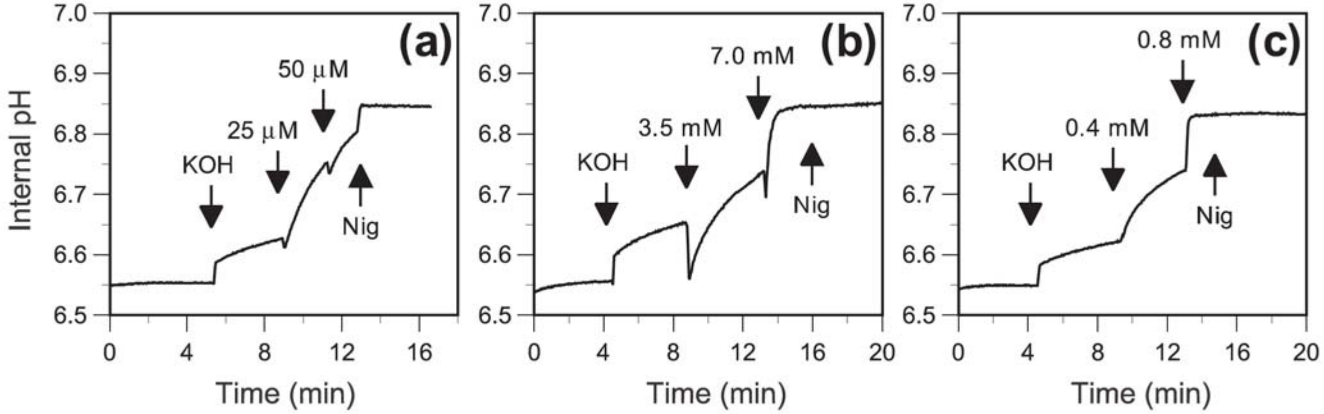
(a)
(b)
(c)
Internal pH
Time (min)
KOH
25 µM
50 µM
Nig
3.5 mM
7.0 mM
0.4 mM
0.8 mM

Fig. 5.

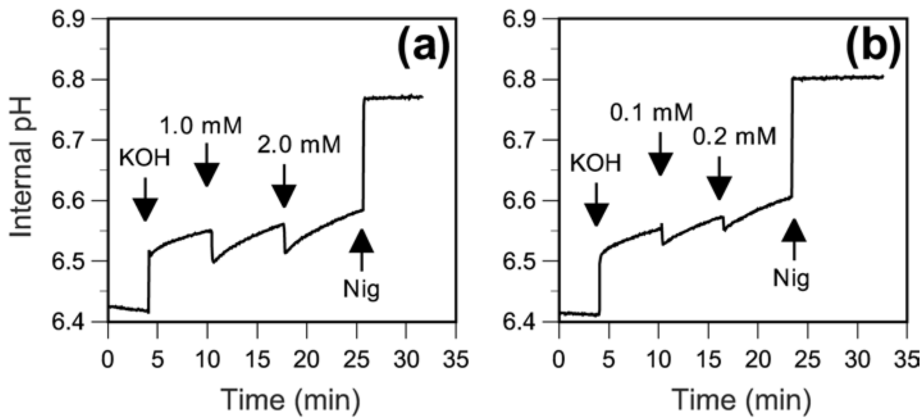
(a)
Internal pH
KOH
1.0 mM
2.0 mM
Nig
Time (min)
(b)
KOH
0.1 mM
0.2 mM
Nig
Time (min)

Fig. 6

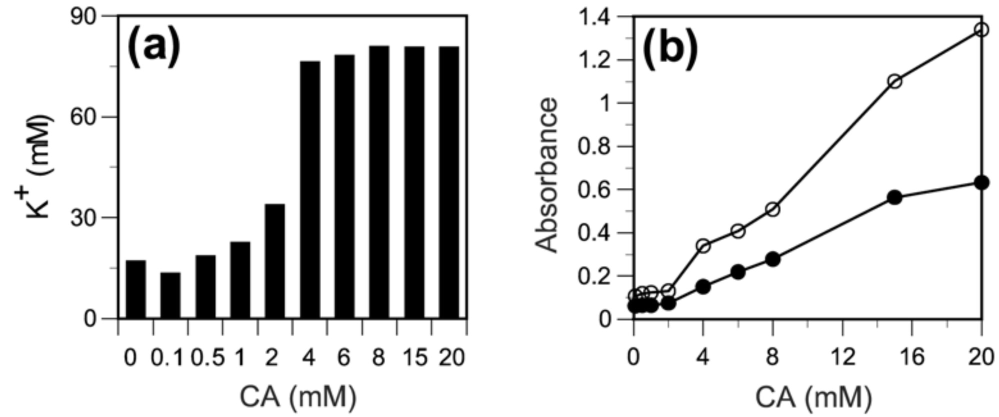
(a)
K+ (mM)
0
30
60
90
0
0.1
0.5
1
2
4
6
8
15
20
CA (mM)
(b)
Absorbance
0
0.2
0.4
0.6
0.8
1
1.2
1.4
0
4
8
12
16
20
CA (mM)

Fig. 7